Research article

LUMINESCENCE
The Journal of Biological and Chemical Luminescence

Received: 6 December 2012, Revised: 5 March 2013, Accepted: 11 March 2013 Published online in Wiley Online Library: 17 May 2013

(wileyonlinelibrary.com) DOI 10.1002/bio.2520

A novel phosphorescence sensor for Co^{2+} ion based on Mn-doped ZnS quantum dots

Wei Bian,[a,b] Jing Ma,[b] Qiaoling Liu,[a] Yanli Wei,[a] Yingfu Li,[a] Chuan Dong[a] and Shaomin Shuang[a]*

ABSTRACT: *N*-acetyl-L-cysteine-capped Mn-doped ZnS quantum dots (QDs) were prepared by hydrothermal methods. It could emit phosphorescence at 583 nm with the excitation wavelength at 315 nm. The phosphorescence intensity of QDs could be quenched dramatically by increasing the concentration of Co^{2+} ion. The novel phosphorescence sensor based on *N*-acetyl-L-cysteine-capped QDs was developed for detecting Co^{2+} ion with a linear dynamic range of 1.25×10^{-6}–3.25×10^{-5} M. The limit of detection and RSD were 6.0×10^{-8} M and 2.3%, respectively. Interference experiments showed excellent selectivity over numerous cations such as alkali, alkaline earth and transitional metal ions. The possible quenching mechanism was also examined by phosphorescence decays. The proposed phosphorescence method was further applied to the trace determination of Co^{2+} ion in tap and pond water samples with recoveries of 97.75–103.32%. Copyright © 2013 John Wiley & Sons, Ltd.

Keywords: doped quantum dots; phosphorescence sensor; cobalt ion

Introduction

Cobalt plays an important role in the metabolism of iron and synthesis of hemoglobin. Chronic cobalt deficiency is one of the main risk factors for cardiovascular disease and vitiligo. An excess of cobalt causes vasodilatation, flushing and cardiomyopathy in humans and animals (1,2). There has been intense interest in the study of cobalt in environmental and biological samples. Many methods have been used for the determination of Co^{2+} ion, including cyclic voltammetry (3), spectrophotometry (4), electrothermal atomic absorption spectrometry (5) and fluorimetry (6). However, these methods suffer from limitations of long extraction time, expensive cost of maintenance, complicated operation and strong interferences from various ions (7). Hence, facile and selective methods for Co^{2+} ion are highly desirable.

In recent years, a determination method based on water-soluble quantum dots (QDs) as markers of fluorescence and room temperature phosphorescence aroused extensive interest (8). Compared with traditional organic dyes, QDs had many unique properties such as high luminescence efficiency, wide and continuous excitation spectrum, narrow and symmetric emission spectrum, tunable color, and high photochemical stability, (9). Their application extended to detecting all kinds of analytes, including ions (10–12), small molecules (13–15) and biological macromolecules (16–19).

QDs properties of phosphorescence are to some extent superior to that of fluorescence. The longer lifetime and emission wavelength of phosphorescence could easily avoid interference from autofluorescence emission and scattered light over fluorescence. Hu and Zhang (20) reviewed the research progress in transition metal or rare earth doped phosphorescence nanomaterials. Snee's group (21) found that ZnSe/ZnMnS/ZnS QDs could emit phosphorescence in aqueous solution. This discovery implied the potential application of phosphorescence properties of QDs in biomedicine. Subsequently, the phosphorescence application potential of QDs was developed. Room temperature phosphorescence (RTP) of dopants and host semiconductors in a number of doped semiconductor systems have emerged. Tu *et al.* (22) synthesized amine-capped Mn-doped ZnS nanocrystals for fluorescence analysis. Yan group (23–26) extended such nanocrystals to RTP sensing DNA, persistent organic pollutants in water, enoxacin and glucose in biological fluids. Wu and Fan (27) also reported doped ZnS QDs as phosphorescence sensors for detecting raceanisodamie hydrochloride and atropine sulfate in biological fluids.

In the present study, water-soluble Mn-doped ZnS QDs using *N*-acetyl-L-cysteine (NAC) as a stabilizer were synthetized. The phosphorescence of QDs was greatly quenched by Co^{2+} ion at pH 8.5 phosphate buffer solution (PBS). Interestingly, RTP of Mn-doped ZnS QDs was found to respond sensitively to Co^{2+} ion. A novel phosphorescence sensor for the determination of Co^{2+} ion was developed without any deoxidants and heavy atom perturbers. The method was applied successfully to the determination of Co^{2+} ion in tap and pond water samples with satisfactory results, and the quenching mechanism and phosphorescence decay discussed.

* Correspondence to: Shaomin Shuang, Research Center of Environmental Science and Engineering, Department of Chemistry, Shanxi University, Taiyuan 030006, People's Republic of China. E-mail: smshuang@sxu.edu.cn

[a] Department of Chemistry and Chemical Engineering, Research Center of Environmental Science and Engineering, Shanxi University, Taiyuan, 030006, People's Republic of China

[b] School of Basic Medical Science, Shanxi Medical University, Taiyuan, 030001, People's Republic of China

Experimental section

Chemicals

NAC was obtained from Aladdin Chemicals. $ZnSO_4{\cdot}7H_2O$, $MnCl_2{\cdot}4H_2O$ and $Na_2S{\cdot}9H_2O$ were obtained from Tianjin Chemical Reagent Company (Tianjin, China). Other analytical grade chemicals were purchased from Beijing Chemical Reagent Company (Beijing, China). All of the chemicals were used as received without further purification. Purified water from a Milli-Q-RO4 water purification system (Millipore, Bedford, MA, USA) with a resistivity higher than 18 MΩ/cm was used to prepare all solutions. PBS 0.1 M was prepared by mixing standard solutions of 0.1 M Na_2HPO_4 and 0.1 M NaH_2PO_4. The pH was adjusted with 0.1 M H_3PO_4 and NaOH solutions.

Apparatus

The absorption and fluorescence measurements were performed with a UV-265 spectrophotometer (Shimadzu Corporation, KYOTO, JAPAN), and F-4500 spectrofluorometer (Hitachi High-Technologies Corporation, Ibarakiken, Japan), respectively. Excitation and emission bandwidths were both set at 10 nm. A 150 W xenon arc lamp was used as the excitation light source. A standard 1 cm quartz cell was used. pH values were measured using a Model pHS-3C pH meter (Shanghai Rex Instrument Factory, Shanghai, China). Transmission electron microscopy (TEM) image obtained using a Japanese model JEM-1011 at 100 kV. Fourier transform infrared (IR) spectra were acquired on a Nicolet Magna-IR 750 spectrometer (Thermo Fisher, Waltham, MA, USA) in the wave number range 500–4000/cm at a resolution of 4/cm. The nanocomposite samples were mixed with KBr and pressed to form KBr plates. Phosphorescence lifetime measurements were performed on an Edinburgh FLS920 spectrometer (Edinburgh, UK). The hydrodynamic diameter was measured by dynamic light scattering (DLS) using a Malvern Autosizer ZS90 spectrometer (Melvin City, UK). All experiments were carried out at 20 ± 1 °C.

Synthesis of water-soluble *N*-acetyl-L-cysteine-capped Mn-doped ZnS quantum dots

Mn-doped ZnS QDs were synthesized according to a reported method with some modification (Scheme 1) (28). Fifty milliliters of 0.03 M NAC, 5 mL of 0.1 M $ZnSO_4$ and 1.5 mL of 0.01 M $MnCl_2$ were added to a three-necked flask. The mixed solution was adjusted to pH ≈ 11 with 2 M NaOH and stirred under nitrogen at room temperature for 40 min. Five milliliters of 0.1 M Na_2S were then quickly injected into the solution. The mixture was stirred for 40 min, and then the solution was aged at 50 °C under air for 2.5 h to form NAC-capped Mn-doped ZnS QDs. The QDs were precipitated with ethanol, separated by centrifuging, washed with ethanol and dried in a vacuum. The prepared QDs powder is highly soluble in water.

Measurement procedure

A certain amount of Mn-doped ZnS powder was dispersed in deionized water and a solution of 50 mg/L was obtained. Different concentrations of Co^{2+} ion were added into 0.8 mL QDs solution (50 mg/L) and diluted to 2.0 mL with PBS aqueous solution of pH 8.5. The fluorescence spectra were obtained with excitation wavelength at 315 nm. The scan speed was 1200 nm/min and band-slits of both excitation and emission were set as 10 nm. The phosphorescence measurements were carried out with an excitation wavelength of 315 nm when the spectrophotometer was set in the phosphorescence mode. The slit widths of excitation and emission were 10 nm. Four milliliters of 50 mg/L Mn-doped ZnS QDs solution, 5.0 mL of PBS (pH 8.5) and a given concentration of Co^{2+} ion standard solution were sequentially added to a 10 mL calibrated test-tube. The mixture was then diluted to 10 mL with high purity water and mixed thoroughly.

Procedure for water samples pretreatment

Tap water was collected from our laboratory and pond water was gathered from a small pond at Shanxi University. The sample collected was first filtered through qualitative filter paper to remove suspended matter, impurities, etc., and then boiled for 5 min to remove chlorine and dissolved gases. After that, water samples were spiked with standard Co^{2+} ion at different concentration levels, then the sample was diluted within the working linear range and analyzed with the proposed method.

Results and discussion

Characterization of *N*-acetyl-L-cysteine-capped Mn-doped ZnS quantum dots

The NAC-capped Mn-doped ZnS nanocrystalline was characterized by TEM, DLS, IR, absorption, fluorescence and phosphorescence spectra. The TEM image and DLS revealed Mn-doped ZnS QDs with spherical shape and almost uniform diameter ≈ 10 nm (Figs 1 and 2). The IR spectra of NAC and QDs capped with NAC are displayed in Fig. 3. It was obvious that the absorption band at 2570/cm, which is ascribed to the sulfhydryl group,

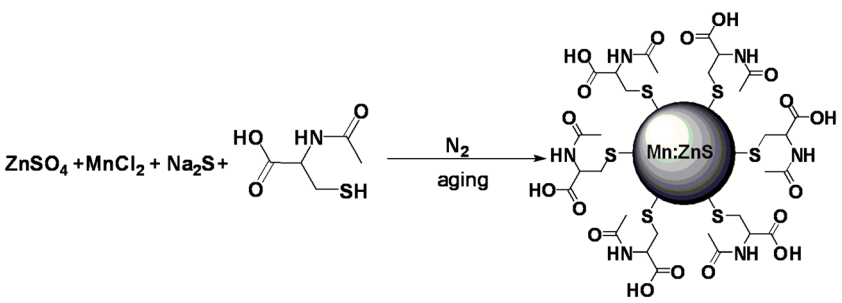

Scheme 1. Synthesis of Mn-doped ZnS quantum dots.

LUMINESCENCE
The Journal of Biological and Chemical Luminescence

disappeared in the spectrum of QDs-NAC. The stretch vibrations of the carboxyl group of NAC at 1710/cm shifted to 1590/cm after binding to QDs. The UV absorption peak was at 291 nm,

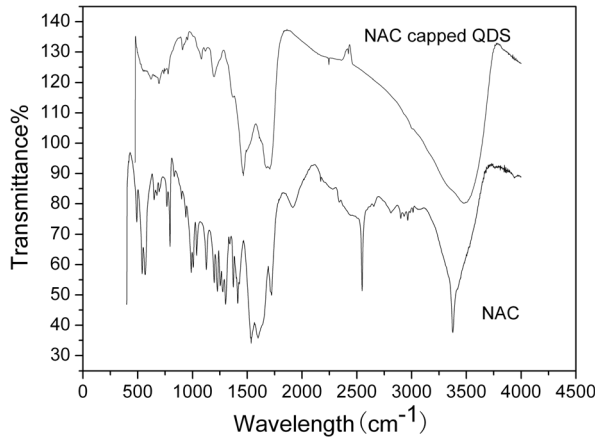

Figure 1. Fourier transform infrared spectra of NAC-capped Mn-doped ZnS QDs and pure NAC. NAC, *N*-acetyl-L-cysteine; QDs, quantum dots.

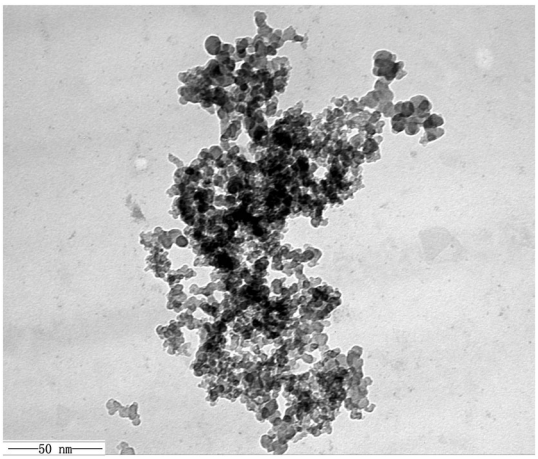

Figure 2. Transmission electron microscopy pattern of *N*-acetyl-L-cysteine-capped Mn-doped ZnS quantum dots.

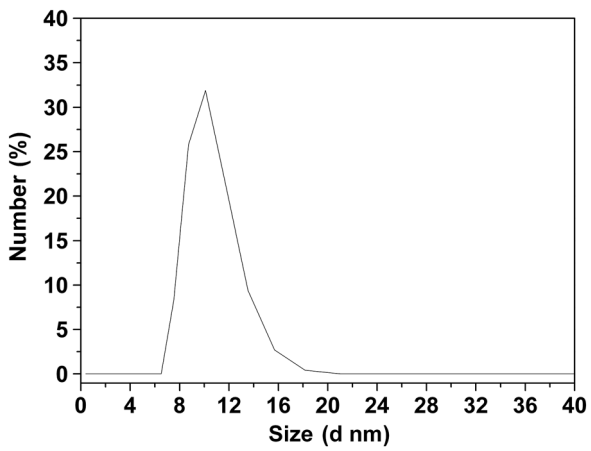

Figure 3. Size distribution by volume of *N*-acetyl-L-cysteine-capped Mn-doped ZnS Hydrosol. (Quantum dots concentration: 20 mg/L, average size is 10 nm). d, diameter.

which displayed the band gap of Mn-doped ZnS nanocrystal particles. It could be concluded that NAC had bound to the surface of QDs. In comparison with the phase material of ZnS whose absorption peak was at 341 nm, the absorption peak blue shifted 50 nm. The phenomena demonstrated that Mn-doped ZnS QDs possessed a quantum confinement effect (Fig. 4) (29). When the excitation wavelength was set at 315 nm, both fluorescence emission peaks were at 450 nm and 583 nm, respectively (Fig. 5). The weak fluorescence emission at 450 nm was derived from the defect-related emission of ZnS. The phosphorescence spectra exhibited a single emission peak at 583 nm with the excitation wavelength at 315 nm (Fig. 6). The strong fluorescence emission peak and phosphorescence emission peak at 583 nm belonged to the $^4T_1$-$^6A_1$ transition of Mn^{2+} impurity, which indicated Mn^{2+} entered into the ZnS lattice to form Mn-doped ZnS QDs. Nevertheless, the green fluorescence of the ZnS phase was not observed, which belonged to energy transfer from ZnS QDs to Mn^{2+} (30).

Analytical merits of phosphorescence detection of Co^{2+} ion

Mn-doped ZnS QDs could emit strong phosphorescence at 583 nm with excitation at 315 nm, which could be quenched dramatically by Co^{2+} ion in suitable buffer media (Fig. 8).

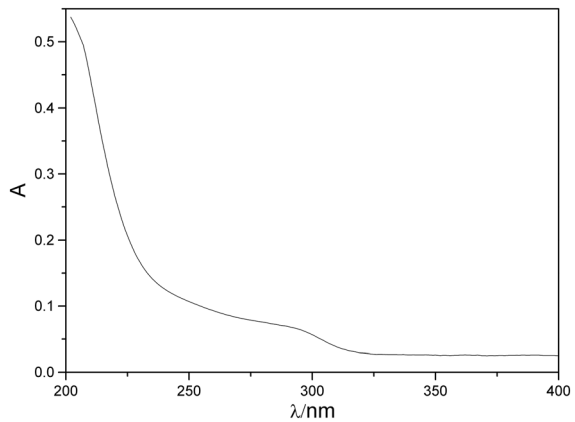

Figure 4. The absorbtion spectra of *N*-acetyl-L-cysteine-capped Mn-doped ZnS quantum dots (40 mg/L). A, absorbance.

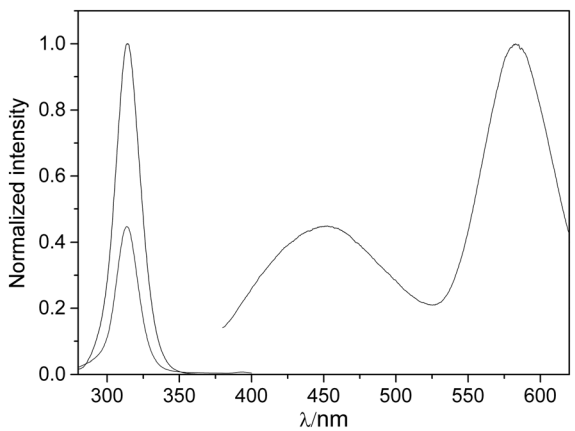

Figure 5. Excitation and emission fluorescent spectra of *N*-acetyl-L-cysteine-capped Mn-doped ZnS quantum dots (20 mg/L).

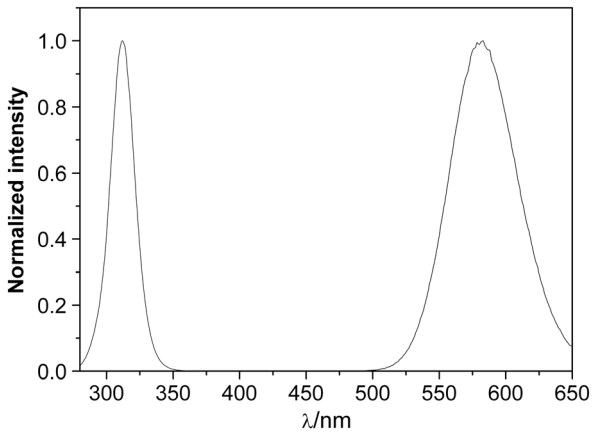

Figure 6. Excitation and emission phosphorescence spectra of *N*-acetyl-L-cysteine-capped Mn-doped ZnS quantum dots (20 mg/L).

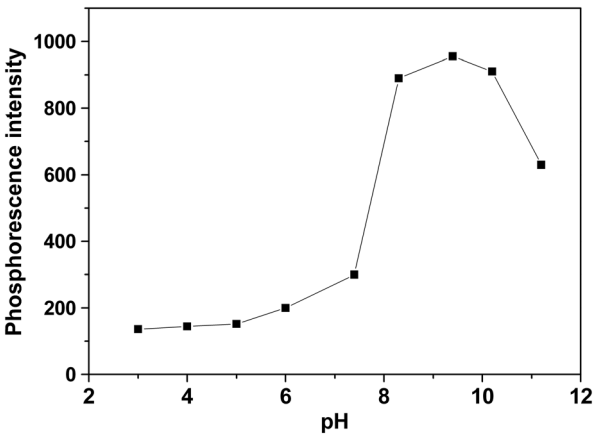

Figure 7. Effect of pH on phosphorescence intensity of *N*-acetyl-L-cysteine-capped Mn-doped ZnS quantum dots (quantum dots concentration: 20 mg/L, λex: 315 nm).

Meanwhile, no discernible changes in the maximum or shape of the phosphorescence spectrum were observed during the quenching. The interaction between Mn-doped ZnS QDs and Co^{2+} ion was strongly influenced by the pH of the solution. The phosphorescence intensity stabilized in the pH range 8.3–10.0. The low phosphorescence intensity in acid medium could be ascribed to dissociation of the QDs and capping agent because of prolongation of the surface-binding sulfhydryl compounds. Along with the increase in pH, deprotonation of the thiol group in the capping molecule occurred. It enhanced the covalent bond between QDs and the capping molecule. This process removed the surface defects of QDs and resulted in an increase in phosphorescence intensity with increased pH. A further increase in pH then elevated a negative charge on the carboxylic acid group of the capping agent, which facilitated dispersion of QDs, producing high phosphorescence intensity. However, the net phosphorescence intensity decreased at higher pH due to the precipitation formation of metal hydroxides (Fig. 7) (31,32), hence pH8.5 PBS buffer was selected. It should be noted that $Co(OH)_2$ was not formed when mixing PBS (pH 8.5) buffer solution with Co^{2+} ion, even at millimolar concentrations. Thus, it is proposed that the phosphorescence quenching is not from the formation of $Co(OH)_2$ on the surface of the QDs.

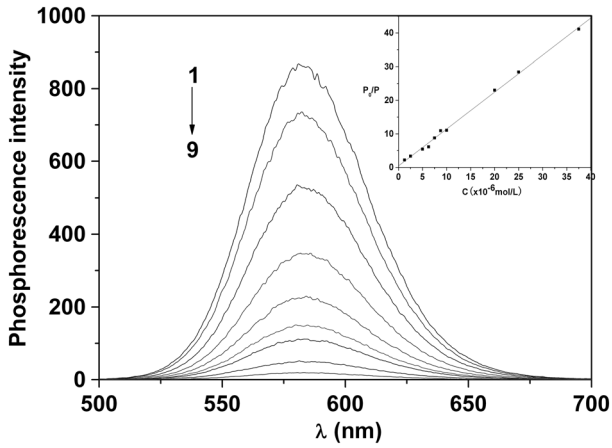

Figure 8. Effect of Co^{2+} ion concentration on phosphorescence intensity of Mn-doped ZnS quantum dots. The concentration of Co^{2+} ion (1–9) were: 0, 2.0, 4.0, 6.0, 8.0, 10.0, 15.0, 25.0 and 37.5 μM. Inset graph is Stern–Volmer plot of the Co(II) concentration dependence of phosphorescence intensity of *N*-acetyl-L-cysteine-capped Mn-doped ZnS quantum dots. (Quantum dots concentration: 20 mg/L, λex: 315 nm, in pH 8.5, PBS).

The results showed that the presence of trace amounts of Co^{2+} ion gave rise to an obvious quenching of the emission of Mn-doped ZnS QDs, and the phosphorescence was nearly completely quenched in the presence of 3.75×10^{-5} M Co^{2+} ion. This suggested a strong interaction between Co^{2+} ion and NAC-capped Mn-doped ZnS QDs.

The effect of Co^{2+} ion concentration on the phosphorescence of NAC-capped Mn-doped ZnS QDs is shown in Fig. 8. The phosphorescence intensity of NAC-capped Mn-doped ZnS QDs was dramatically decreased with the increase of Co^{2+} ion concentration. Thus, a quantitative detection of Co^{2+} ion based on phosphorescence quenching is possible. The analytical characteristics of Co^{2+} ion based on the phosphorescence quenching of Mn-doped ZnS QDs had been exploited. The change of phosphorescence intensity ΔP as a function of the Co^{2+} ion concentration was linear in the range of 1.25×10^{-6}–3.25×10^{-5} M with the linear regression equation of $\Delta P = 52.32\ [Co^{2+}] + 59.093$ ($r = 0.9982$) (C: value in the magnitude of 10^{-6} M). The limit of detection was 6.0×10^{-8} M (S/N = 3) and the relative SD was 2.3% ($n = 11$).

Selectivity of the phosphorescence sensing system based on Mn-doped ZnS quantum dots

Selectivity was a very important parameter to evaluate the performance of the phosphorescence sensing system. The effect of various mental ions on the phosphorescence spectra of Mn-doped ZnS QDs was examined. The phosphorescence intensity of NAC-capped Mn-doped ZnS QDs was quenched enormously in the presence of 1.0×10^{-5} M of Co^{2+} ion, whereas some other metal ions, including alkali, alkaline earth and transition metal ions led to very slight or even no phosphorescence intensity change upon the presence of 1.0×10^{-4} M of individual cations, as shown in Fig. 9(A). This result indicated that the QDs-based sensor showed good selectivity toward Co^{2+} ion over other competitive cations.

The impacts of some coexisting cations on Co^{2+} ion sensing were also determined. The phosphorescence response of the sensing system toward Co^{2+} ion in the presence of some other metal ions was shown in Fig. 9(B). The coexistence of most

LUMINESCENCE
The Journal of Biological and Chemical Luminescence

selected metal ions does not interfere with Co^{2+} ion binding to the QDs, indicating that these coexistent ions had negligible interfering effect on Co^{2+} ion sensing by the doped QDs. Thus, Co^{2+} ion selective binding could take place in the presence of most of the competitive coexisting metal ions.

Study on the quenching process

Up to now, a variety of processes could contribute to phosphorescence quenching, including energy transfer, excited state reactions, complex formation and collisional quenching (33–36). The latter two processes are often referred to as static and dynamic quenching. Static quenching showed that quencher and phosphorescence substance in the ground state generated non-emitting complexes which lead to a decrease in the phosphorescence intensity of phosphors. This process followed equation (1):

$$1/(P_0 - P) = 1/P_0 + K_{LB}/(P_0[Q]) \quad (1)$$

Where P_0 and P were the phosphorescence intensity in the absence and presence of quencher, respectively. K_{LB} was complex formation constant (37). In static quenching, the RTP lifetime was unchangeable. Dynamic quenching was the interaction between the quencher and the excited state of the phosphorescence material, which caused a decrease in the phosphorescence intensity of phosphors with a concomitant shortening in the RTP lifetime. This process followed the Stern–Volmer equation (2):

$$P_0/P = 1 + K_{sv}[Q] \ \ or \ \ \tau_0/\tau = 1 + k_q\tau_0[Q] \quad (2)$$

Where K_{sv} was the phosphorescence quenching constant, which was related to the quenching efficiency of the quencher, and [Q] was the concentration of the quencher ([Co^{2+}]). k_q was the phosphorescence quenching constant, and τ and τ_0 were the lifetime of phosphorescence in the presence and absence of quencher (38,39). The phosphorescence data were then analyzed by plotting P_0/P versus [Co^{2+}].The resulting plot as shown in Fig. 8, exhibited a linear relationship in the range of 1.25×10^{-6}–3.75×10^{-5} M ($R = 0.9989$), K_{sv}, calculated by linear regression of the plots, was 2.42×10^6/M. A plot of P_0/P as a function of [Q] indicated that quenching of the luminescence of QDs was probably attributed to the dynamic quenching. To

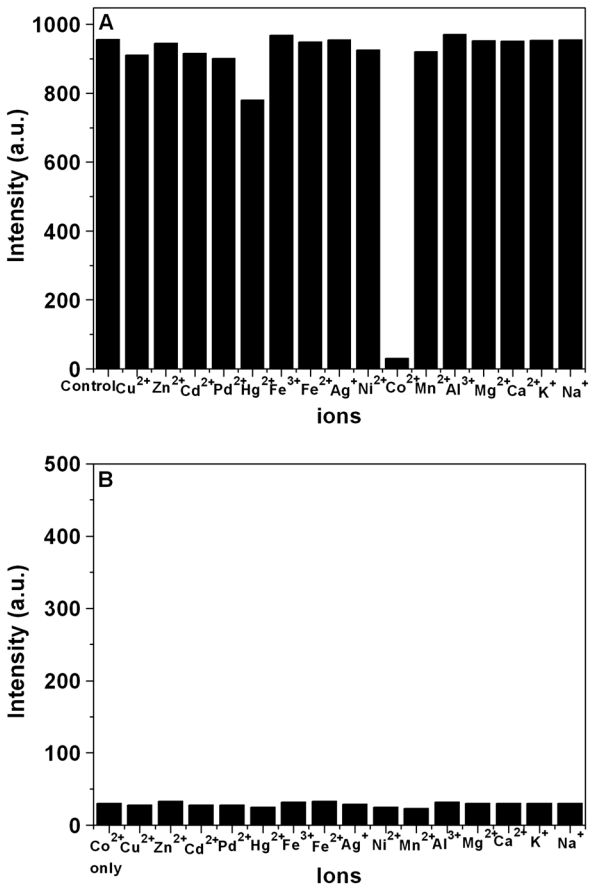

Figure 9. (A) Phosphorescence intensity change of Mn-doped ZnS quantum dots upon addition of other different metal ions (100 μM), Co^{2+} ion (10 μM), respectively. (B) Phosphorescence intensity change of Mn-doped ZnS quantum dots in the presence of 10 μM of Co^{2+} ion with 100 μM of various coexisting metal cations respectively. Co^{2+} ion only: in the presence of 10 μM. (λex: 315 nm, in pH 8.5, PBS, quantum dots concentration: 20 mg /L).

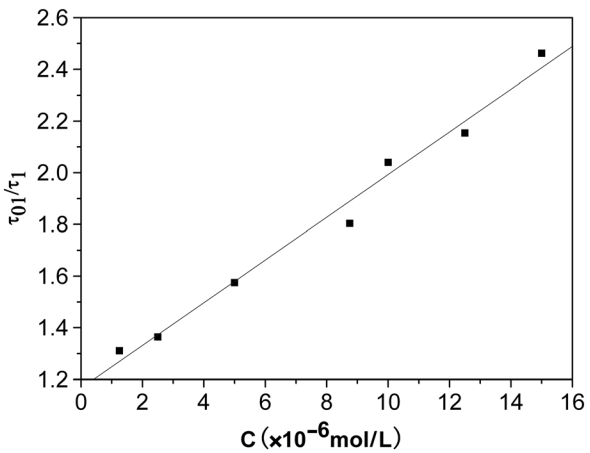

Figure 10. τ_{01}/τ_1 of *N*-acetyl-L-cysteine-capped Mn-doped ZnS quantum dots vs [Co^{2+}] linear fitting figure. (Quantum dots concentration: 20 mg/L, λex: 315 nm, in pH 8.5, PBS).

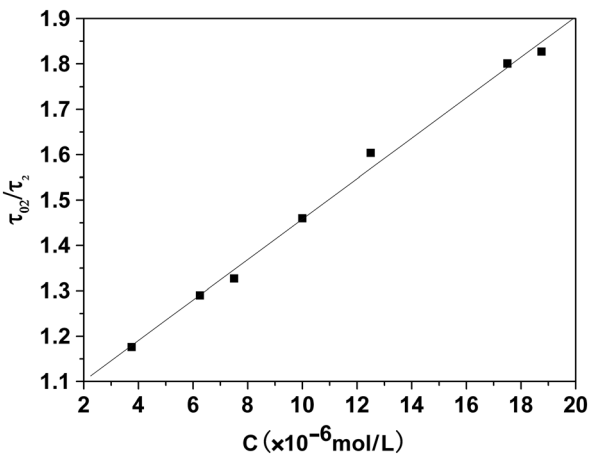

Figure 11. τ_{02}/τ_2 of *N*-acetyl-L-cysteine-capped Mn-doped ZnS quantum dots vs [Co^{2+}] linear fitting figure. (Quantum dots concentration: 20 mg/L, λex: 315 nm, in pH 8.5, PBS).

Table 1. Analytical results for determination of Co^{2+} in water samples

Water samples	Found (M)	Added (μM)	Found ($n = 3$) (μM)	Recovery (%)	Relative SD (%)
Tap water	Not found	4.00	3.92	98.00	1.80
		8.00	7.82	97.75	2.05
		25.00	25.83	103.32	2.12
Pond water	Not found	4.00	3.95	98.75	1.66
		8.00	8.21	102.63	2.15
		25.00	24.56	98.24	2.02

further confirm the quenching mechanism, the phosphorescence decays of the Mn-doped ZnS QDs at different concentrations of Co^{2+} ion had been recorded and the decays were fitted with the equation $\tau_0/\tau = 1 + k_q\tau_0[Q]$. There existed two lifetimes of τ_1 and τ_2 with fast and slow decays in the absence of the Co^{2+} ion. Upon addition of the Co^{2+} ion, the values for τ_1 and τ_2 were found to decrease dramatically, respectively, with relative weights of 12% and 88%. The values were further analyzed by plotting τ_0/τ versus $[Co^{2+}]$. The resulting plot exhibited a good linear relationship. k_q were 3.47×10^7/M per s and 6.61×10^6/M per s, respectively (Figs 10 and 11). The values of the phosphorescence decays also further confirmed that the mechanism involved dynamic quenching.

Analytical application of the sensor in water samples

To demonstrate the potential of the phosphorescence sensor, NAC-capped Mn-doped ZnS QDs were used in the analysis of different environmental water samples. Tap water and pond water were used to carry out these studies. Then, standard Co (II) solutions were added to the water samples and analyzed by the standard addition method. The results (Table 1) showed that the recoveries of Co^{2+} ion for these samples were in the range 97.75–103.32%. These results demonstrated that the designed phosphorescence sensor was reliable and practical for the detection of Co^{2+} ion in different environmental water samples.

Conclusions

NAC-capped Mn-doped ZnS QDs were successfully synthesized in aqueous medium, characterized by TEM, DLS, IR, absorption, fluorescence and phosphorescence spectra and exhibited strong phosphorescence at 583 nm. The phosphorescence could be quenched dramatically in the presence of Co^{2+} ion. A novel phosphorescence method for the determination of Co^{2+} ion was developed. Excellent selectivity was obtained for Co^{2+} ion over a large number of cations such as alkali, alkaline earth and transitional metal ions. The quenching process involved dynamic quenching. The mechanism of interaction between Mn-doped ZnS QDs and Co^{2+} ion will be studied in more detail in the future. Based on the low cost and low toxicity of Mn-doped ZnS QDs, future work will be directed to the design of biosensors for biological systems.

Acknowledgments

Financial supports from the National Natural Science Foundation of China (Nos. 21175086 and 21175087), Shanxi Province Hundred Talent Project Support, Shanxi college students' innovative fund (Nos. 2011116 and 2012103), Shanxi medical university students' innovation fund (No. 201231) and 331 Early Career Researcher Grant of Shanxi Medical University Medical School Foundation.

References

1. Bar-Or D, Lau E, Rao N, Bampos N, Winkler JV, Curtis CG. Reduction in the cobalt binding capacity of human albumin with myocardial ischemia. Ann Emerg Med 1999;34(4):S56.
2. Yuzefovsky AI, Lonardo RF, Wang MH, Michel RG. Determination of ultra-trace amounts of cobalt in ocean water by laser-excited atomic fluorescence spectrometry in a graphite electrothermal atomizer with semi on-line flow injection preconcentration. J Anal Atom Spectrom 1994;9(11):1195–202.
3. Korolczuk M, Moroziewicz A, Grabarczyk M, Paluszek K. Determination of traces of cobalt in the presence of nioxime and cetyltrimethylammonium bromide by adsorptive stripping voltammetry. Talanta 2005;65(4):1003–7.
4. Rohilla R, Gupta U. Simultaneous determination of Cobalt (II) and Nickel (II) by first order derivative spectrophotometry in micellar media. eJ Chem 2012;9(3):1357–63.
5. Berton P, Martinis EM, Martinez LD, Wuilloud RG. Selective determination of inorganic cobalt in nutritional supplements by ultrasound-assisted temperature-controlled ionic liquid dispersive liquid phase microextraction and electrothermal atomic absorption spectrometry. Anal Chim Acta 2012;713:56–62.
6. Wang P, Li Z, Lv GC, Zhou HP, Hou C, Sun WY, Tian YP. Zinc(II) complex with teirpyridine derivative ligand as "on-off" type fluorescent probe for cobalt(II) and nickel(II) ions. Inorg Chem Commun 2012;18:87–91.
7. Taher MA, Puri BK. Column preconcentration of cobalt with the ion pair of 2-nitroso1-naphthol-4-sulfonic acid-tetradecyldimethylbenzylammonium chloride supported on naphthalene using second-derivative spectrophotometry. Analyst 1995;120(5):1589–92.
8. Medintz IL, Uyeda HT, Goldman ER, Mattoussi H. Quantum dot bioconjugates for imaging, labelling and sensing. Nat Mater 2005;4:435–46.
9. Suyver JF, Wuister SF, Kelly JJ. Synthesis and photoluminescence of nanocrystalline ZnS:Mn^{2+}. Nano Lett 2001;1(8):429–33.
10. Jin WJ, Fernández-Argüelles MT, Costa-Fernández JM, Pereiro R, Sanz-Medel A. Photoactivated luminescent CdSe quantum dots as sensitive cyanide probes in aqueous solutions. Chem Commun 2005;7:883–5.
11. Fernández-Argüelles MT, Jin WJ, Costa-Fernández JM, Pereiro R, Sanz-Medel A. Surface-modified CdSe quantum dots for the sensitive and selective determination of Cu(II) in aqueous solutions by luminescent measurements. Anal Chim Acta 2005;549:20–5.
12. Li HB, Zhang Y, Wang XQ, Xiong DJ, Bai YQ. Calixarene capped quantum dots as luminescent probes for Hg^{2+} ions. Mater Lett 2007;61(7):1474–7.
13. Huang CP, Li YK, Chen TM. A highly sensitive system for urea detection by using CdSe/ZnS core-shell quantum dots. Biosens Bioelectron 2007;22(8):1835–8.
14. Liang JG, Huang S, Zeng DY, He ZK, Ji XH, Ai XP, Yang HX. CdSe quantum dots as luminescent probes for spironolactone determination. Talanta 2006;69(1):126–30.
15. Cordes DB, Gamsey S, Singaram B. Fluorescent quantum dots with boronic acid substituted viologens to sense glucose in aqueous solution. Angew Chem 2006;45(23):3829–32.

16. Wang LY, Wang L, Gao F,Yu ZY, Wu ZM. Application of functionalized CdS nanoparticles as fluorescence probe in the determination of nucleic acids. Analyst 2002;127(7):977–80.
17. Chen XD, Dong YP, Fan L, Yang DC. Fluorescence for the ultrasensitive detection of peptides with functionalized nano-ZnS. Anal Chim Acta 2007;582(2):281–7.
18. Chen HQ, Wang L, Liu Y, Wu WL, Liang AN, Zhang XL. Preparation of a novel composite particles and its application in the fluorescent detection of proteins. Anal Bioanal Chem 2006;385(8):1457–61.
19. Yao HQ, Zhang Y, Xiao F, Xia ZY, Rao JH. QD-BRET based highly sensitive detection of proteases. Angew Chem 2007;46(23):4346–9.
20. Hu H, Zhang WH. Synthesis and properties of transition metals and rare-earth metals doped ZnS nanoparticles. Opt Mater 2006;28(5):536–50.
21. Thakar R, Chen YC, Snee PT. Efficient emission from core /(doped) shell nanoparticles: applications for chemical sensing. Nano Lett 2007;7(11):3429–32.
22. Tu R, Liu BH, Wang ZY, Gao DM, Wang F, Fang QL, Zhang ZP. Amine-capped ZnS-Mn^{2+} nanocrystals for fluorescence detection of trace TNT explosive. Anal Chem 2008;80(9):3458–65.
23. He Y, Yan XP. Mn-doped ZnS quantum dots/methyl violet nanohybrids for room temperature phosphorescence sensing of DNA. Sci China Chem 2011;54(8):1254–9.
24. Wang HF, He Y, Ji TR, Yan XP. Surface molecular imprinting on Mn-doped ZnS quantum dots for room-temperature phosphorescence optosensing of pentachlorophenol in water. Anal Chem 2009;81(4):1615–21.
25. Wu P, He Y, Wang HF, Yan XP. Conjugation of glucose oxidase onto Mn-doped ZnS quantum dots for phosphorescent sensing of glucose in biological fluids. Anal Chem 2010;82(4):1427–33.
26. He Y, Wang HF, Yan XP. Exploring Mn-doped ZnS quantum dots for the room-temperature phosphorescence detection of enoxacin in biological fluids. Anal Chem 2008;80(10):3832–7.
27. Wu H, Fan ZF. Mn-doped ZnS quantum dots for the room-temperature phosphorescence detection of raceanisodamine hydrochloride and atropine sulfate in biological fluids. Spectrochim Acta Part A 2012,90:131–4.
28. Zhuang JQ, Zhang XD, Wang G, Li DM, Yang WS, Li TJ. Synthesis of water-soluble ZnS:Mn^{2+} nanocrystals by using mercaptopropionic acid as stabilizer. J Mater Chem 2003;13(7):1853–7.
29. Brus LE. Electron-electron and electron-hole interactions in small semiconductor crystallites: the size dependence of the lowest excited electronic state. J Chem Phys 1984;80(9):4403–9.
30. Chung JH, Ah CS, Jang DJ. Formation and distinctive decay times of surface- and lattice-bound Mn^{2+} impurity luminescence in ZnS nanoparticles. J Phys Chem B 2001;105(19):4128–32.
31. Gao M, Kirstein S, Moehwald H, Rogach AL, Kornowski A, Eychmuller A, Weller H. Strongly photoluminescent CdTe nanocrystals by proper surface modification. J Phys Chem B 1998;102(43):8360–3.
32. Chen ST, Zhang XL, Zhang QH, Hou XM, Zhou Q, Yan JL. CdSe quantum dots decorated by mercaptosuccinic acid as fluorescence probe for Cu^{2+}. J Lumin 2011;131:947–51.
33. Isarov AV, Chrysochoos J. Optical and photochemical properties of nonstoichiometric cadmium sulfide nanoparticles: surface modification with copper (II) ions. Langmuir 1997;13(12):3142–9.
34. Liu FC, Chen YM, Lin JH, Tseng WL. Synthesis of highly fluorescent glutathione-capped $Zn_xHg_{1-x}Se$ quantum dot and its application for sensing copper ion. J Colloid Interface Sci 2009;337(2):414–9.
35. Liu J, Lu Y. A DNAzyme catalytic beacon sensor for paramagnetic Cu^{2+} ions in aqueous solution with high sensitivity and selectivity. J Am Chem Soc 2007;129(32):9838–9.
36. Chen JL, Zheng AF, Gao YC, He CY, Wu GH, Chen YC, Kai XM, Zhu CQ. Functionalized CdS quantum dots-based luminescence probe for detection of heavy and transition metal ions in aqueous solution. Spectrochim Acta Part A 2008;69(3):1044–52.
37. Sauer K, Scheer H, Sauer P. Förster transfer calculations based on crystal structure data from Agmenellum quadruplicatum C-phycocyanin. Photochem Photobiol 1987;46(3):427–40.
38. Lakowicz JR. *Principles of fluorescence spectroscopy*, 2nd rev edn. New York: Kluwer. Academic/Plenum Publishers, 1999.
39. Lakowicz JR, Weber G. Quenching of fluorescence by oxygen – A probe for structural fluctuations in macromolecules. Biochemistry 1973;12(21):4161–70.